ChemComm

Accepted Manuscript

This is an *Accepted Manuscript*, which has been through the Royal Society of Chemistry peer review process and has been accepted for publication.

Accepted Manuscripts are published online shortly after acceptance, before technical editing, formatting and proof reading. Using this free service, authors can make their results available to the community, in citable form, before we publish the edited article. We will replace this *Accepted Manuscript* with the edited and formatted *Advance Article* as soon as it is available.

You can find more information about *Accepted Manuscripts* in the **Information for Authors**.

Journal Name

ARTICLE TYPE

Synthesis and *In Vitro* Assessment of a Bifunctional Closomer Probe for Fluorine (^{19}F) Magnetic Resonance and Optical Bimodal Cellular Imaging†

Lalit N. Goswami, Aslam A. Khan, Satish S. Jalisatgi and M. Frederick Hawthorne*

The design, synthesis and *in vitro* assessment of a bifunctional imaging probe for dual fluorine (^{19}F) magnetic resonance spectroscopy (^{19}F-MRS) and fluorescence detection is reported. Eleven copies of 3, 5-Bis(trifluoromethyl)phenyl 10 and a single copy of a sulforhodamine-B were covalently attached to a *closo*-B$_{12}$$^{2-}$ -core via suitable linkers. The ^{19}F-MRS and fluorescence imaging shows that, this novel bimodal imaging probe was readily taken up by the cells *in vitro* after co-incubation.

15

The use of multiple imaging techniques in conjunction with one another has begun to gain popularity propelled by the development of hybrid scanners with multiple imaging capabilities (PET-CT, SPECT-CT, Optical-CT, MRI-PET, MRI- 20 Optical and other).[1] These multimodal imaging systems can be used to diagnose and image cancerous lesions in the early stages of disease progression and can effectively change the clinical outcome of the treatment regime. They are thus believed to be the future of medical imaging. Nuclear imaging (PET and 25 SPECT) is a well-developed area in medicine and therefore significant research has been focused on designing bimodal imaging probes combining nuclear imaging with radio (CT, X-ray) or MR or optical imaging capabilities.[2] However, due to the drawbacks associated with the nuclear imaging probes (i.e. 30 ionizing radiation, half-life and special handling), an alternative imaging modality with comparable sensitivity is desirable. The combination of MRI and optical imaging can be advantageous and very logical. MRI can provide detailed anatomic imaging, while optical imaging can provide the molecular imaging during 35 image guided procedures.

^{1}H and ^{19}F provide very sensitive nuclei for MRI.[3-4] While there are several dual function ^{1}H MRI/optical probes that have been developed,[5] there are only a few examples of dual ^{19}F MRI/optical imaging probes.[6-7] The clinically used ^{1}H MRI 40 probes are dominated by Gd^{3+}-chelates. However there is a high risk of nephrogenic systemic fibrosis (NSF) when using Gd^{3+} in patients suffering from renal disfunction or failure.[8] Recently the ^{19}F nuclide has gained popularity among researchers as a valuable

International Institute of Nano and Molecular Medicine, School of 45 *Medicine, University of Missouri, Columbia, Missouri 65211-3450, USA. E-mail: hawthornem@missouri.edu*

† Electronic supplementary information (ESI) available: Experimental procedures and characterization details.

clinical imaging modality.[9-10] 50 The NMR sensitivity of ^{19}F is 0.83 relative to ^{1}H, has a 100% natural isotopic abundance ratio, has a large chemical shift range (300 ppm), and ^{19}F MRI probes are often more stable (covalent) than the Gd^{3+} based chelates (non-covalent) used in ^{1}H MRI. Also, the human body itself provides a negligible endogenous ^{19}F 55 MRI signal. One general challenge in the development of MRI/optical bimodal probes is the difference in the detection sensitivity between MRI (low sensitivity) and optical imaging (high sensitivity). A much higher concentration of the MRI probe is required compared to the optical counterpart. This problem can 60 be addressed with the use of a multifunctional dendritic core such as a per-hydroxylated icosahedral [*closo*-B$_{12}$(OH)$_{12}$]$^{2-}$ ion (**1**). Each B-OH vertex of this ion can be attached to pre-determined payloads to generate attractive molecular scaffolds, termed as "*Closomers*" (Figure **1**). The synthesis of a bimodal imaging 65 probe requires the presence of heterobifunctionalized linker arms on the same scaffold to permit concurrent attachment of differing payloads on a single core using orthogonal chemistries. To this end, we have developed a synthetic methodology to differentiate a single B-OH vertex of [*closo*-B$_{12}$(OH)$_{12}$]$^{2-}$ to produce [*closo*- 70 B$_{12}$(OR)(OH)$_{11}$]$^{2-}$.[11] The synthetic strategy has been successfully utilized towards the preparation of α$_v$β$_3$ integrin-targeted closomer for high performance MRI applications.[12] This methodology permits the covalent attachment of a single optical probe, while the remaining 11 vertices can carry payloads of ^{19}F 75 nuclei, (Figure **1**).

Fig. 1 Schematic representation of organic synthesis on an icosahedral *closo*-B$_{12}$$^{2-}$ surface.
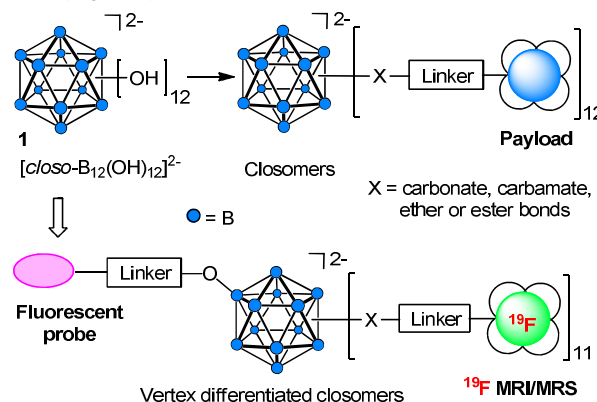
This combination can increase the effectiveness of a bimodal ^{19}F MRI/optical imaging probe by providing high fluorous content per molecule. Herein, we describe the synthesis and *in vitro* studies of the first bifunctional imaging probe derived from an icosahedral *closo*-B$_{12}$$^{2-}$ -core for applications in bimodal cellular imaging (^{19}F MRI and optical).

In this novel design, the entire fluorous payload is attached to the central *closo*-B$_{12}$$^{2-}$ -core via carbamate linkages (B-OCO-NH-) using tetraethyleneglycol (TEG) linkers and thereby generates a single ^{19}F NMR signal for all 66 ^{19}F nuclei, a much desired criteria for successful ^{19}F-MRS/MRI (Scheme-1). First, the 4-nitrophenyl carbonate closomer **2** was prepared according to the reported literature procedure.[11] Next, **2** was reacted with the amine terminated 3, 5-bis(trifluoromethyl)benzoic acid derivative **S3** (ESI). The resulting 11-fold carbamate closomer **3** was purified by size-exclusion column chromatography on Lipophilic Sephadex LH-20 using MeOH as eluent and characterized by NMR and HRMS analysis (ESI). Finally, the synthesis of bifunctional closomer **^{19}F-B$_{12}$-FL** was accomplished by attaching the alkyne terminated sulforhodamine-B derivative **S5** (ESI) to the azide functionality of the lone vertex of closomer **3** via an azide-alkyne click reaction. The **^{19}F-B$_{12}$-FL** was purified by size-exclusion column chromatography on Lipophilic Sephadex LH-20 using MeOH as the eluent and was characterized by NMR and HRMS analysis.
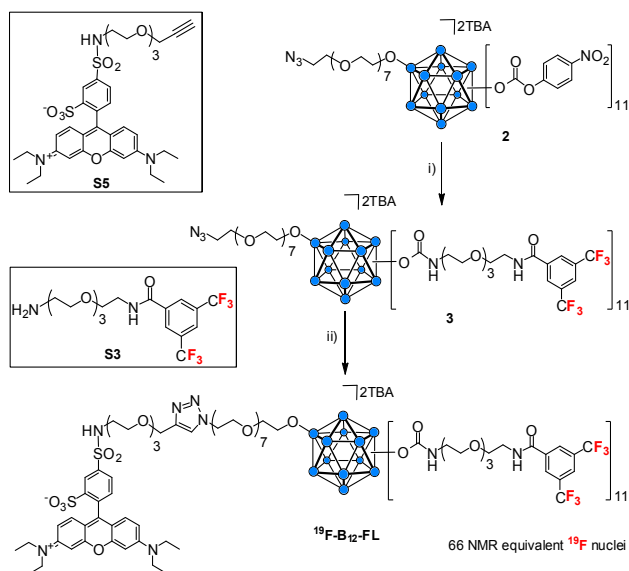
Scheme 1 Synthesis of **^{19}F-B$_{12}$-FL**. *Reagents and conditions*: i) **S3**, ACN, RT, 3 days, 84%. ii) **S5**, CuI, DIPEA, ACN-THF, RT, 12 h, 91%.

The cell labeling experiments were carried out by performing a time dependent cellular uptake study to determine the average time for maximum cellular uptake of **^{19}F-B$_{12}$-FL**. The A549 cells (human lung cancer cell line) were co-incubated with a 100 μM solution of **^{19}F-B$_{12}$-FL** for various time points. Cellular uptake of **^{19}F-B$_{12}$-FL** was then investigated using ^{19}F NMR (Figure **2**) and fluorescence spectroscopy (Figure **S1**, SI) of the lysed cell pellets. In ^{19}F NMR spectroscopy of the lysed cell pellets, the uptake of **^{19}F-B$_{12}$-FL** was observed by a characteristic peak at -61 ppm (referenced to peak for TFA at -76 ppm). The

intracellular concentration of **^{19}F-B$_{12}$-FL** reached a maxima after 1h of incubation, although there was no significant difference in cell uptake between 30 min and 1h.
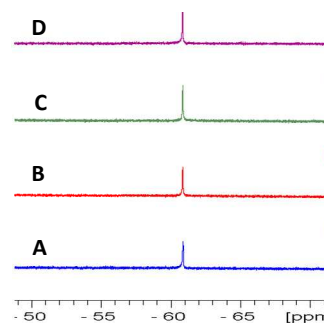
Fig. 2 Time dependent uptake of **^{19}F-B$_{12}$-FL** by human A549 cells. Figure shows ^{19}F NMR signal intensity of cell lysates post incubation of 100 μM of **^{19}F-B$_{12}$-FL** at various time-points. (A) 5 min, (B) 30 min, (C) 1 h, (D) 3 h.

Next, the dose dependent cellular uptake of **^{19}F-B$_{12}$-FL** was determined. Cells (A549) were co-incubated with various concentrations (5-80 μM) of **^{19}F-B$_{12}$-FL** for a period of 1h. Cells were lysed and the lysates were analyzed using fluorescence (Figure **3**) and ^{19}F NMR spectroscopy (Figure **4**). As expected, the fluorescence spectroscopy showed cellular uptake of **^{19}F-B$_{12}$-FL** even at the lowest dose of 5 μM. Even though the sensitivity of ^{19}F MRI is low as compared to optical imaging techniques, a very high payload of ^{19}F nuclei (total 66) in **^{19}F-B$_{12}$-FL** was able to display the cellular uptake of the **^{19}F-B$_{12}$-FL** as a single peak at -61 ppm (Figure **4**). A linear relationship between incubation concentration and cellular uptake of **^{19}F-B$_{12}$-FL** was found via both fluorescence and by ^{19}F NMR spectroscopy, demonstrating the utility of **^{19}F-B$_{12}$-FL** as a bimodal imaging probe.
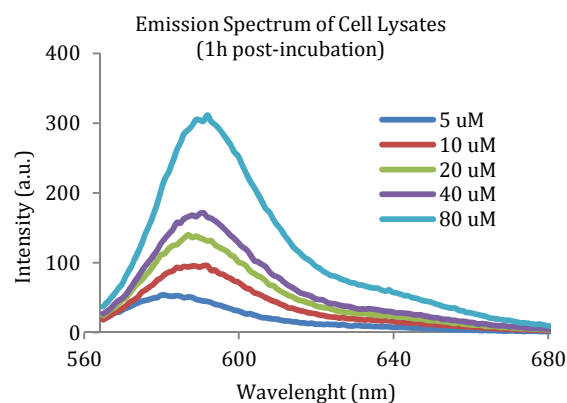
Fig. 3 Dose dependent labeling of human A549 cells with bimodal probe **^{19}F-B$_{12}$-FL**. Figure shows emission spectra of cell lysates 1h post incubation of **^{19}F-B$_{12}$-FL** at various concentrations.

The cell viability MTT assay of **^{19}F-B$_{12}$-FL** was examined on four different cell lines including both human and mouse cancer cell lines. Of all four cell lines, EMT-6 mouse breast cancer cells, DLD1 colorectal adenocarcinoma cells and T47D cells were tested at 0.1, 1.0, 10.0, 50.0 and 100 μM while A549 cells were tested at 1.0, 10.0, and 100 μM concentrations.

For all concentrations tested, the cell viability was >85% compared to the untreated control (Figure 5).
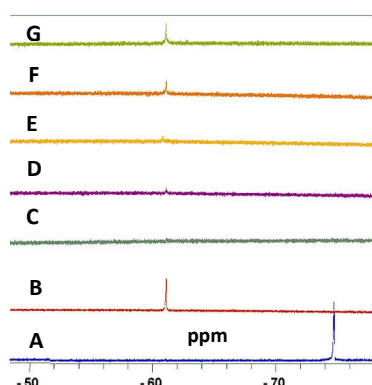
5 **Fig. 4** Dose dependent labeling of human A549 cells with bimodal probe **^{19}F-B$_{12}$-FL**. Figure shows ^{19}F NMR signal intensity of cell lysates 1h post incubation of **^{19}F-B$_{12}$-FL** at various concentrations. (A) TFA reference, -76 ppm, (B) **^{19}F-B$_{12}$-FL** reference, -61 ppm, (C-G) Cells incubated with 5, 10, 20, 40, 80 μM of **^{19}F-B$_{12}$-FL** respectively, -61 ppm.

10
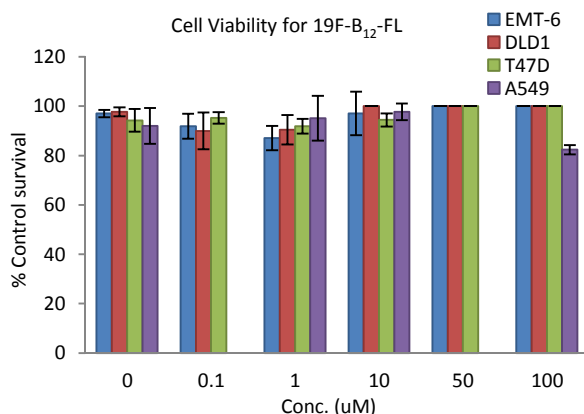
Fig. 5 Cell viability assessment of bimodal probe **^{19}F-B$_{12}$-FL** by MTT assay at various concentrations (0.1-100 μM) in four different cell lines.

15 Finally, intracellular localization studies of this bimodal probe were performed by co-incubating 10 μM of **^{19}F-B$_{12}$-FL** with T47D human breast cancer cells for 1h (Figure **6**).
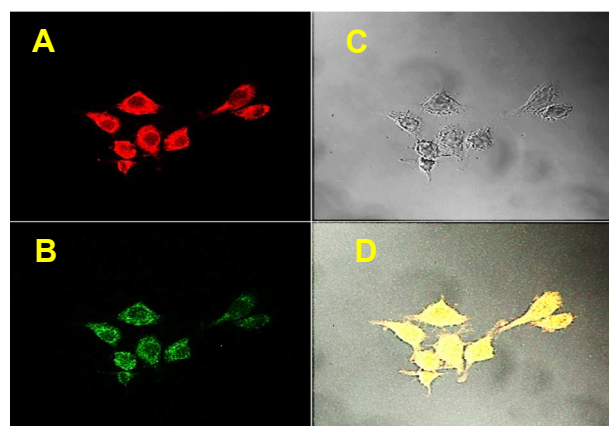
20 **Fig. 6** Fluorescence microscopy images of human T47D cells labeled with bimodal probe **^{19}F-B$_{12}$-FL** and lysotracker green. Panels A-D show intracellular localization of 10 μM of **^{19}F-B$_{12}$-FL** 1h post incubation. Panels: (A) Red, **^{19}F-B$_{12}$-FL**. (B) Green, lysotracker green. (C) Light. (D) Merge.

25 The confocal microscopy images show localization of **^{19}F-B$_{12}$-FL** in the cytoplasm. The co-localization of **^{19}F-B$_{12}$-FL** with lysotracker green further indicates that the **^{19}F-B$_{12}$-FL** was predominantly localized in the lysosomes.

In summary, we have synthesized a highly fluorous 30 bifunctional cellular imaging probe, **^{19}F-B$_{12}$-FL**, based on a vertex-differentiated *closo*-B$_{12}$$^{2-}$ core that relies on ^{19}F-MRS and fluorescence detection. Since the entire fluorous payload originates from an identical starting point (B-O-), the **^{19}F-B$_{12}$-FL** generates a single ^{19}F NMR signal for all 66 fluorine atoms, a 35 condition appropriate for ^{19}F MRI. The *in vitro* assessment shows that **^{19}F-B$_{12}$-FL** is nontoxic to cells and is readily taken up by the cells after co-incubation for a short period of time (<1h). The *in vitro* cell localization studies show that the probes localize preferentially in lysosomes. These *in vitro* results highlight the 40 potential of **^{19}F-B$_{12}$-FL** as a cellular imaging agent and warrant the further evaluation *in vivo* for toxicity, bio-distribution and imaging capabilities. Nevertheless, in conjugation with target specific ligands this bifunctional imaging platform would further open up the possibility of imaging (^{19}F-MR and fluorescence) of 45 cancerous lesions and other abnormalities *in vivo*.

Notes and references

1. A. Louie, *Chem. Rev.,* 2010, **110**, 3146.
50 2. H. Kobayashi, M. R. Longmire, M. Ogawa and P. L. Choyke, *Chem. Soc. Rev.*, 2011, **40**, 4626.
3. J. Ruiz-Cabello, B. P. Barnett, P. A. Bottomley and J. W.M. Bulte, *NMR Biomed.* 2011, **24**: 114.
4. J. Yu, R. R. Hallac, S. Chiguru and R. P. Mason, *Progress in* 55 *Nuclear Magnetic Resonance Spectroscopy*, 2013, **70**, 25.
5. M. F. Penet, M. Mikhaylova, C. Li, B. Krishnamachary, K. Glunde, A. P. Pathak and Z. M. Bhujwalla, *Future Med. Chem.*, 2010, **2**, 975.
6. J. M. Janjic, M. Srinivas, D. K. Kadayakkara and E. T. Ahrens, *J.* 60 *Am. Chem. Soc.*, 2008, **130**, 2832.
7. B. E. Rolfe, I. Blakey, O. Squires, H. Peng, N. R. B. Boase, C. Alexander, P. G. Parsons, G. M. Boyle, A. K. Whittaker and K. J. Thurecht, *J. Am. Chem. Soc.*, 2014, **136**, 2413.
8. J. Idée, M. Port, C. Medina, E. Lancelot, E. Fayoux, S. Ballet and C. 65 Corot, *Toxicology*, 2008, **248**, 77.
9. Z. Jiang, X. Liu, E. Jeong, and Y. B. Yu, *Angew. Chem. Int. Ed.*, 2009, **48**, 4755.
10. J. C. Knight, P. G. Edwards and S. J. Paisey, *RSC Advances*, 2011, **1**, 1415.
70 11. L. N. Goswami, Z. H. Houston, S. J. Sarma, H. Li, S. S. Jalisatgi and M. F. Hawthorne, *J. Org. Chem.*, 2012, **77**, 11333.
12. L. N. Goswami, L. Ma, Q. Cai, S. J. Sarma, S. S. Jalisatgi and M. F. Hawthorne, *Inorg. Chem.* 2013, **52**, 1701.

75

80

85